Mitochondrial matrix Ca^{2+} as an intrinsic signal regulating mitochondrial motility in axons

Karen T. Chang[a,1], Robert F. Niescier[b], and Kyung-Tai Min[b,1]

[a]Zilkha Neurogenetic Institute and Department of Cell and Neurobiology, University of Southern California, Los Angeles, CA 90033; and [b]Department of Biology, Indiana University, Bloomington, IN 47405

Edited by Ronald D. Vale, University of California, San Francisco, CA, and approved August 3, 2011 (received for review April 29, 2011)

The proper distribution of mitochondria is particularly vital for neurons because of their polarized structure and high energy demand. Mitochondria in axons constantly move in response to physiological needs, but signals that regulate mitochondrial movement are not well understood. Aside from producing ATP, Ca^{2+} buffering is another main function of mitochondria. Activities of many enzymes in mitochondria are also Ca^{2+}-dependent, suggesting that intramitochondrial Ca^{2+} concentration is important for mitochondrial functions. Here, we report that mitochondrial motility in axons is actively regulated by mitochondrial matrix Ca^{2+}. Ca^{2+} entry through the mitochondrial Ca^{2+} uniporter modulates mitochondrial transport, and mitochondrial Ca^{2+} content correlates inversely with the speed of mitochondrial movement. Furthermore, the miro1 protein plays a role in Ca^{2+} uptake into the mitochondria, which subsequently affects mitochondrial movement.

Mitochondria are dynamic organelles that constantly move within cells and undergo morphological changes in response to physiological needs (1–3). In neurons, mitochondria are abundantly present throughout different subcellular compartments. The machineries and signals that transport mitochondria from the cell body (where they are synthesized) to the terminal need to be carefully regulated because of the highly polarized structure and lengthy axon of a neuron (4–6). Defects in transport of mitochondria can cause deleterious effects on mitochondrial functions in different parts of neurons, and hence affect neuronal survival and function (2, 3). Recent efforts to investigate mitochondrial transportation have provided significant new information regarding mitochondrial mobility, especially the mechanical components that modulate mitochondrial transport; however, it remains unclear whether intrinsic signals inside of mitochondria also actively regulate mitochondrial movement.

Mitochondrial transport is mediated by interactions of the mitochondrial adaptor proteins to the kinesin and dynein motors, as well as binding of the motor proteins to the cytoskeleton track (7, 8). It was posited that cytoplasmic Ca^{2+} level is a key regulator of mitochondrial trafficking in axons and dendrites, and that intracellular Ca^{2+} influx impedes mitochondrial movement by affecting the overall interactions between the mitochondrial adaptor, motor, and cytoskeleton track (9, 10). Two different mechanisms for Ca^{2+}-mediated stop in mitochondrial trafficking were proposed. Wang and Schwarz suggested that Ca^{2+} binding to the EF hand motif of the mitochondrial adaptor protein miro1 recruits kinesin-1 motor and, hence, derails kinesin-1 from the microtubule track, thereby stopping mitochondrial transportation in axons (10). Macaskill et al. proposed that following Ca^{2+} influx induced by glutamate or neuronal activity, Ca^{2+} binding to the EF hand motif of the miro1 protein causes miro1 to dissociate from the kinesin-1 motor, and hence halts mitochondrial movement (11). Although the mechanisms proposed for this Ca^{2+}-induced arrest in mitochondrial movement are different, both groups agree that cytoplasmic Ca^{2+} elevation and its subsequent binding to the miro1 protein are key events regulating mitochondrial motility in neurons.

Cytoplasmic Ca^{2+} has been deemed important for mitochondrial motility in neurons; however, the relationship between mitochondrial Ca^{2+} content and movement has not been established. It also remains unclear whether mitochondria play a passive or active role in their own transport. Aside from the endoplasmic reticulum, mitochondria are another main source of Ca^{2+} buffering within the cell. Following intracellular Ca^{2+} elevation, mitochondria rapidly take up and accumulate Ca^{2+} to maintain cellular Ca^{2+} homeostasis (12). Studies also have shown that Ca^{2+} uptake into mitochondria occurs through the mitochondrial Ca^{2+} uniporter (12, 13), and that mitochondrial Ca^{2+} influx can increase ATP production by activating the TCA cycle, as well as enhance the activities of the electron transport-chain enzymes and the ATP synthase complex (14–17). Nevertheless, the relationship between mitochondrial energetic status and mitochondrial movement remains controversial. A report showed that anterogradely moving mitochondria have higher membrane potential than those moving retrogradely (18), yet another group found no difference between the membrane potentials of mitochondria moving in opposite directions or between the stationary and mobile mitochondria (19). The parameters within mitochondria associated with changes in the pattern of mitochondrial motility thus remain unclear. Because Ca^{2+} in mitochondria is associated with various mitochondrial functions, we hypothesized that mitochondrial Ca^{2+} may act as a signal that allows mitochondria to actively regulate their own mobility. Here, we show Ca^{2+} influx through the mitochondrial Ca^{2+} uniporter modulates mitochondrial transport, and that mitochondrial Ca^{2+} content correlated inversely with the speed of mitochondrial movement. Furthermore, we demonstrate that the miro1 mutant modulates mitochondrial trafficking by altering the amount of Ca^{2+} influx into the mitochondria in axons of hippocampal neurons. Taken together, our results imply that mitochondrial matrix Ca^{2+} is an intrinsic signal that actively regulates mitochondrial transportation in neurons.

Results and Discussion

Visualization of Mitochondrial Ca^{2+} in Axons. Detecting small changes in the level of Ca^{2+} within mitochondria of living neurons have been challenging because of the lack of subcellular specificity provided by synthetic Ca^{2+} indicators. To test the hypothesis that internal mitochondrial Ca^{2+} modulates mitochondrial motility, we targeted a genetically encoded GFP-based fluorescent Ca^{2+} indicator, Case12, to the mitochondria. This targeting was achieved by inserting a mitochondrial signal peptide into the N terminus of the Case12 protein (mito-Case12). Case12 protein allows linear detection of Ca^{2+} ion concentration within the physiological range and its binding to Ca^{2+} is rapid and reversible, thus making real-time detection of changes in Ca^{2+} level within a cell possible (20, 21). Mito-Case12 colocalized with mito-RFP in transfected hippocampal neurons (Fig. 1*A*, Fig. S1 *A* and *C*), thus confirming that mito-Case12 is indeed targeted to the mitochondria. Next, to test the ability of mito-Case12 to

Author contributions: K.T.C. and K.-T.M. designed research; K.T.C. and R.F.N. performed research; K.T.C. and K.-T.M. analyzed data; and K.T.C. and K.-T.M. wrote the paper.

The authors declare no conflict of interest.

This article is a PNAS Direct Submission.

[1]To whom correspondence may be addressed. E-mail: kyumin@indiana.edu or changkt@usc.edu.

This article contains supporting information online at www.pnas.org/lookup/suppl/doi:10.1073/pnas.1106862108/-/DCSupplemental.

respond to increases in Ca^{2+} content, we treated hippocampal neurons containing mito-Case12 and mito-RFP with calcimycin, a Ca^{2+} ionophore (Fig. S1*A*). Following calcimycin treatment, the green fluorescence intensity of mito-Case12 increased significantly within seconds in mitochondria, but the mito-RFP signal remained constant (Fig. S1 *A* and *B*). Mito-Case12 signal is dependent on calcium influx into the cell, because calcimycin treatment in calcium-free extracellular solution failed to cause an increase in mito-Case12 signal (Fig. S1 *C* and *D*). To account for the difference in the size of mitochondria and thus the amount of fluorescent protein inside of mitochondria, as well as change in focal plane that could occur over time, we also normalized mito-Case12 labeling intensity to that of mito-RFP intensity. Similar to mito-Case12 signal, normalized mito-Case12:mito-RFP ratio increased following calcimycin treatment. Together, our results suggest that (*i*) mito-Case12 is able to detect Ca^{2+} elevation within mitochondria, and (*ii*) Ca^{2+} is rapidly taken up by mitochondria following intracellular Ca^{2+} elevation.

Mitochondrial Ca^{2+} Content Predicts Mitochondrial Mobility. Having confirmed that mito-Case12 can detect Ca^{2+} elevation inside of mitochondria, we next investigated if mitochondrial Ca^{2+} correlates with mitochondrial movement in axons under normal conditions. To visualize mitochondrial movement and Ca^{2+} content within the mitochondria, time-lapse live imaging of primary hippocampal neurons doubly transfected with mito-RFP and mito-Case12 was performed. Fig. 1*A* shows a kymograph illustrating mitochondrial movement (*x* axis) over time (*y* axis), in which the stationary mitochondria are displayed as straight vertical lines as they are immobile over time, whereas the moving mitochondria are seen as diagonal lines. Interestingly, we noticed that compared with stationary mitochondria, moving mitochondria tend to have lower mito-Case12 fluorescence signal, and hence lower mitochondrial Ca^{2+} content. To minimize for variability caused by drifts in the focal plane as well as differences in size of mitochondria, we normalized mito-Case12 labeling intensity to that of mito-RFP intensity. Fig. 1 *A* and *B* and Fig. S2 show that average mito-Case12:mito-RFP ratio is clearly lower in moving mitochondria (mean = 0.27 ± 0.01), but stationary mitochondria exhibited higher ratio of mito-Case12:mito-RFP (mean = 0.39 ± 0.01), confirming that mitochondria in motion tend to have lower matrix Ca^{2+} content than stationary mitochondria.

As mitochondria move in opposite directions (anterograde vs. retrograde) and with different speed, we next determined if the direction or speed of mitochondrial movement correlates with mitochondrial Ca^{2+} content. Analyses of mitochondria moving in opposite directions showed similar mitochondrial Ca^{2+} content, as determined by the ratio of mito-Case12:mito-RFP (anterograde: 0.24 ± 0.01; retrograde: 0.27 ± 0.02; $P = 0.22$). We also calculated the average speed of individual moving mitochondria over the period of imaging and plotted against the average mito-Case12:mito-RFP ratio. Fig. 1*C* shows that the speed of moving mitochondria is between 0.1 μm/s and 0.58 μm/s, within range of values reported previously for mitochondrial movement seen in axons of hippocampal neurons (7). More importantly, Fig. 1*C* shows that there is a strong correlation between the speed of mitochondrial movement with the level of mitochondrial Ca^{2+}; the lower the

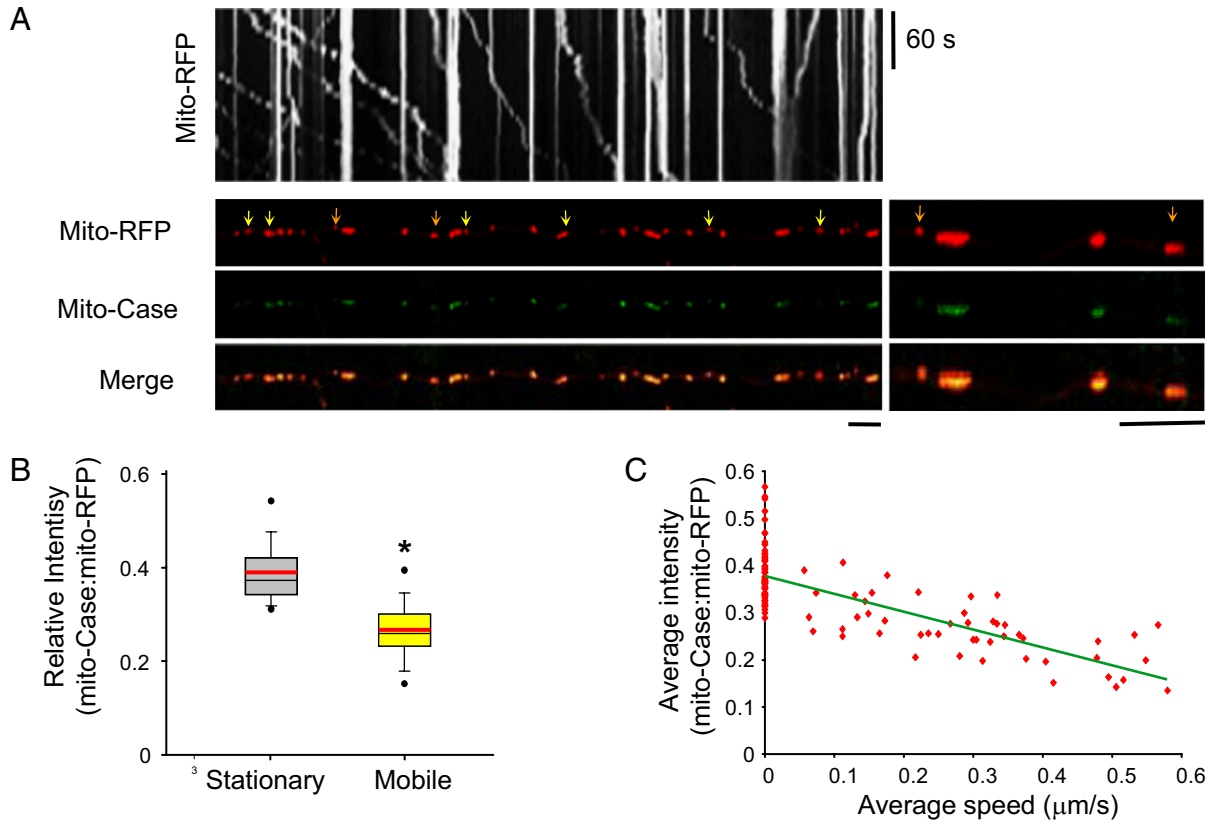

Fig. 1. Moving mitochondria tend to have lower mitochondrial Ca^{2+} signal. (*A*) Kymograph generated from moving mitochondria (*Upper*) and first frame of live imaging of neuron cotransfected with mito-RFP and mito-Case12. Arrows point to moving mitochondria (yellow and orange) and the region magnified on the right is denoted by the orange arrows. (Scale bars, 10 μm.) (*B*) Box plot of the mito-Case12:mito-RFP ratio for stationary and mobile mitochondria. Lower and upper boundaries of the box indicate 25th and 75th percentiles, respectively. The black line in the box represents the median, and the red line represents the mean. Whiskers show 10th and 90th percentiles. Dots above and below the box are showing outliers. $*P = 2 \times 10^{-15}$ (*C*) Average mito-Case12:mito-RFP ratio versus average speed of movement. $R^2 = 0.58$. $n > 150$ mitochondria from 10 axons for *B* and *C*.

mitochondrial matrix Ca^{2+} content, the faster the movement (Pearson correlation coefficient = −0.76 or −0.67, when including or excluding stationary mitochondria, respectively). Our results imply that mitochondrial Ca^{2+} does not influence the directionality of movement; rather, mitochondrial Ca^{2+} content is an important parameter that determines mitochondrial mobility and the speed of mitochondrial movement.

Influx of Ca^{2+} Through the Mitochondrial Ca^{2+} Uniporter Alters Mitochondrial Mobility. Influx of Ca^{2+} into the mitochondrial matrix is gated by the mitochondrial Ca^{2+} uniporter (22, 23), suggesting that it may also play a role in regulating mitochondrial movement. Thus, we next tested the following hypotheses: (*i*) mitochondrial Ca^{2+} uniporter modulates mitochondrial transportation in axons; (*ii*) it is not cytoplasmic Ca^{2+}, but the influx of Ca^{2+} to mitochondrial matrix that ultimately arrests mitochondrial movement. To this end, we examined mitochondrial mobility following either inhibition or activation of the mitochondrial Ca^{2+} uniporter. Treatment of neurons with calcimycin, a Ca^{2+} ionophore, elevates cytoplasmic Ca^{2+} as detected by Case12 protein in the cytoplasm (cyto-Case12) (Fig. 2*A*, *Right*, and Movie S1) and mitochondrial Ca^{2+} as detected by mito-Case12 (Fig. S1). Neurons treated with calcimycin showed immediate Ca^{2+} elevation and stop in mitochondrial movement in axons (Figs. 2 *A* and *D*). This calcimycin-induced stop in mitochondrial movement is dependent on Ca^{2+} influx, because calcimycin treatment in the absence of extracellular calcium failed to pause mitochondrial movement (Fig. S3). To assess whether mitochondrial Ca^{2+} influx into the matrix through the mitochondrial Ca^{2+} uniporter is necessary for Ca^{2+}-induced stop in mitochondrial movement, we first blocked the mitochondrial Ca^{2+} uniporter by treating neurons with RU360 (13), then subsequently challenged it with calcimycin. We reasoned that if the mitochondrial Ca^{2+} uniporter indeed gates mitochondrial Ca^{2+} influx, and hence affect mitochondrial mobility, blocking the mitochondrial Ca^{2+} uniporter would allow mitochondrial movement to persist in the presence of high cytoplasmic Ca^{2+} caused by calcimycin treatment. Fig. 2 *B* and *C* and Movie S2 show that mitochondria incubated with RU360 for 15 min before calcimycin treatment maintained their mobility much longer after calcimycin addition, despite the increase in cytoplasmic Ca^{2+} content indicated by cyto-Case12. Analyses of the percentage of moving mitochondria over the imaging period showed that a significant percentage of mitochondria remained mobile if the neurons were preincubated with RU360 before calcimycin treatment (Fig. 2*D*, normal calcium). However, RU360 only partially restored the percentage of moving mitochondria to normal, thus suggesting that either cytoplasmic Ca^{2+} also contributes, or that RU360 did not completely prevent Ca^{2+} entry into mitochondria. We thus further examined mito-Case12 signal following RU360 and calcimycin treatment (Fig. S4). We found that RU360 delayed Ca^{2+} entry into mitochondria rather than completely abolishing it (Fig. S4), and that mitochondrial movement correlated inversely with mito-Case12 signal elevation, rather than cyto-Case12 profile. To further reduce calcium entry through the mitochondrial Ca^{2+} uniporter, we decreased the level of extracellular Ca^{2+} to 0.18 mM Ca^{2+} (low Ca^{2+}). Calcimycin treatment in low extracellular calcium was sufficient to stop mitochondrial movement (Fig. S5), but it no longer paused mitochondrial movement in neurons pretreated with RU360 (Fig. 2*D* and Fig. S6*A*). Note that we still observed a negligible level of Ca^{2+} influx into the mitochondria after RU360 and calcimycin treatment (Fig. S6*B*; mito-Case12 profile), but at a much slower rate and lower level. This result is consistent with report that RU360 is only partially effective in reducing Ca^{2+} influx through the mitochondrial Ca^{2+} uniporter (24). We also did not observe redistribution in the percentage of mitochondria undergoing anterograde or retrograde transport, suggesting that RU360 treatment or altering Ca^{2+} level does not selectively alter directionality of transport (Fig. S7). Taken together, these results imply that a critical level of calcium influx through the mitochondrial Ca^{2+} uniporter is necessary for the Ca^{2+}-dependent pause in mitochondrial transport in axons.

Next, we tested whether elevation of the mitochondrial matrix Ca^{2+} by activation of the mitochondrial Ca^{2+} uniporter is sufficient to regulate mitochondrial mobility. Neurons containing mito-RFP and mito-Case12 were treated with a drug that activates the mitochondrial Ca^{2+} uniporter, SB202190 (25). SB202190 treatment indeed elevated mitochondrial Ca^{2+} content, as seen by the greater intensity of mito-case12 fluorescence in the kymograph in Fig. 3*A*. Furthermore, the mito-RFP kymograph shows that mitochondria were mobile before SB202190 treatment, but stopped immediately following SB20190 treatment. This sudden change in mitochondrial movement is accompanied by mitochondrial matrix Ca^{2+} elevation (Fig. 3 *A* and *D*). We also plotted the fluorescence ratio of mito-Case12 to mito-RFP before and after SB202190 treatment for the moving mitochondria (Fig. 3*B*). Our results clearly demonstrate that the average Ca^{2+} content in

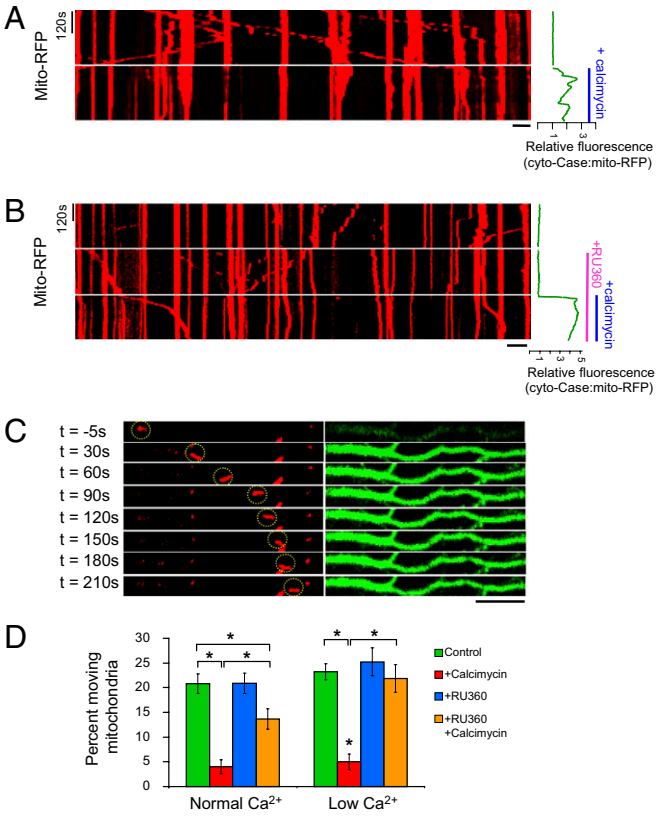

Fig. 2. Blocking Ca^{2+} influx into mitochondria through Ca^{2+}-uniporter delays calcimycin-induced arrest in mitochondrial movement. (*A*) Kymograph of a neuron cotransfected with mito-RFP and cyto-Case12 before and after addition of calcimycin (2 μg/mL). The rise in Ca^{2+} is plotted on the right, shown as relative fluorescence of cyto-Case12:mito-RFP ratio. Immediately after calcimycin treatment and Ca^{2+} elevation, mobile mitochondria became stationary. (*B*) Kymograph showing mitochondrial movement for neurons cotransfected with mito-RFP and cyto-Case12. Relative intensity of cyto-Case12:mito-RFP is shown on the right following RU360 and calcimycin treatments. Ru360 was applied for 15 min before addition of calcimycin, but only the last 5 min of RU360 treatment is shown. (*C*) Mito-RFP (red; *Left*) and cyto-Case12 (green; *Right*) images after 15 min of RU360 and before ($t = -5$ s) and after calcimycin treatment. Despite increase in cytoplasmic Ca^{2+}, mitochondria remained mobile (highlighted by yellow circle). (Scale bars in *A*–*C*, 10 μm.) (*D*) Percentage of moving mitochondria over the 5-min imaging period for each condition. Normal Ca^{2+} indicates 1.8 mM Ca^{2+} and low calcium indicates 0.18 mM Ca^{2+} in the extracellular solution. n = 150–380 mitochondria from at least five axons analyzed. Values represent mean ± SEM; $^*P < 0.01$.

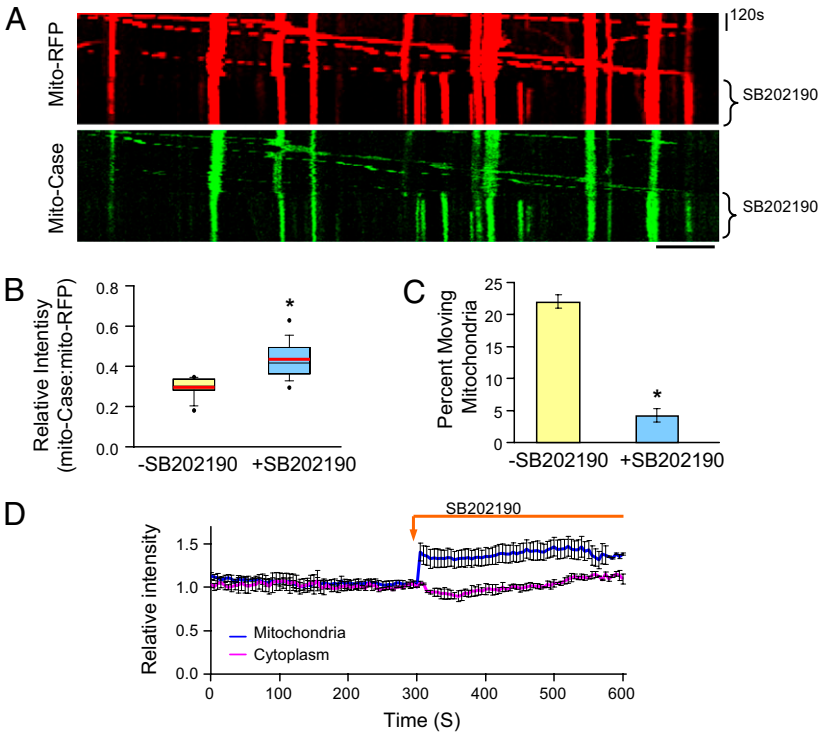

Fig. 3. Mitochondrial Ca^{2+} elevation by activating the mitochondrial Ca^{2+} uniporter is sufficient to stop mitochondrial movement. (*A*) Kymograph of time-lapse images of neuron cotransfected with mito-RFP and mito-Case12 before and after SB202190. (Scale bar, 10 μm.) (*B*) Box plot of mito-Case:mito-RFP intensity ratio before and after SB202190 for the moving mitochondria. n = 40 moving mitochondria from eight axons. Red lines indicate mean. *P = 6 × 10^{-6}. (*C*) Percentage of moving mitochondria before and after SB202190 treatment. n = 200 mitochondria from eight axons. *P = 9 × 10^{-10}. (*D*) SB202190 treatment did not alter cytoplasmic Ca^{2+} level. Relative intensity before and after SB202190 treatment in cytoplasm is measure by Cyto-Case12, and intensity in mitochondria is measured by mito-Case12. To normalize for drifts in z axis during imaging, values were normalized to mito-RFP. Values represent mean ± SEM, n = 8 axons.

the moving mitochondria is lower initially, but increased significantly after activation of mitochondrial Ca^{2+} uniporter with SB202190. Analyses of the percentage of moving mitochondria also confirmed that SB202190 treatment, similar to calcimycin treatment, arrested mitochondrial transport (Fig. 3*C*). Note that SB202190 treatment did not increase cytoplasmic Ca^{2+}, as determined by imaging with cyto-Case12, but significantly elevated mitochondrial Ca^{2+}, as measured by mito-Case12 imaging (Fig. 3*D*). SB202190 has also been shown to inhibit p38 MAPK (26); thus, it is possible that it may influence mitochondrial movement independently of mitochondrial Ca^{2+} elevation. However, the observed inverse relationship between mito-Case12 profile and movement, as well as results obtained using RU360, all support the hypothesis that the mitochondrial Ca^{2+} uniporter regulates mitochondrial movement in axons by gating Ca^{2+} influx into the mitochondrial matrix.

Miro1 Protein Alters Ca^{2+} Entry into Mitochondria. Our findings suggest that mitochondrial Ca^{2+} influx via the mitochondrial Ca^{2+} uniporter actively regulates mitochondrial transport. This result prompted us to re-examine the role of miro1 protein in influencing mitochondrial trafficking and test the possibility that miro1 affects transport by altering mitochondrial Ca^{2+} influx. Previous studies showed that cytoplasmic Ca^{2+} regulates mitochondrial movement mainly by binding to miro1 EF hand domains, thereby altering miro1 interaction with either the kinesin motor or microtubule track (9–11). Mutations in the EF hand domains of miro1 failed to arrest mitochondrial movement despite high intracellular Ca^{2+}, thus highlighting the importance of miro1 in Ca^{2+}-dependent regulation of mitochondrial movement (9–11). We found that transfection of wild-type miro1 ($miro^{wt}$) or miro1 EF hand mutations ($miro^{kk}$) together with mito-RFP and mito-Case12 increased the overall length of mitochondria and the percentage of moving mitochondria, but did not alter the density of mitochondria (number of mitochondria per micrometer) in axons or the average speed of moving mitochondria (Fig. S8). Furthermore, calcimycin treatment failed to stop mitochondrial transport in $miro^{kk}$-transfected neurons, nor did it change the directionality of mitochondrial movement (Fig. S9). These results are consistent with those reported earlier (9–11). Next, we compared the relative levels of mitochondrial Ca^{2+} following calcimycin treatment in control neurons and those transfected with $miro^{wt}$, or $miro^{kk}$, in addition to mito-RFP and mito-Case12. Representative mito-Case12 signals in axons of neurons before and after calcimycin treatment are shown in Fig. 4*A* (pseudocolored). Fig. 4*B* summarizes our findings that mutations in the EF hand domains of miro1 resulted in a significantly lower overall increase in matrix Ca^{2+} level in the axons (fold-change in signal intensity after 3 min of calcimycin treatment, a time point in which the mito-Case12 signal becomes relatively stable are: control, 1.40 ± 0.06; $miro^{wt}$, 1.31 ± 0.03; $miro^{kk}$, 1.11 ± 0.02). Note that the expression of $miro^{wt}$ construct also arrested mitochondrial movement following calcimycin addition (10, 11), and that these axons initially showed Ca^{2+} influx to the same extent as the control (Fig. 4*B*). $Miro^{kk}$ mutant, on the other hand, started with low but gradual Ca^{2+} influx, although never reaching the Ca^{2+} level comparable to calcimycin treated control or $miro^{wt}$-transfected neurons (Fig. 4*B*). To determine if $miro^{kk}$ also influences cytoplasmic Ca^{2+} influx, we examined the cyto-Case12 profile in control and $miro^{kk}$-transfected neurons (Fig. S10). We find that $miro^{kk}$-transfected neurons showed same level of cytoplasmic Ca^{2+} influx as the control. These results imply that mutations in miro1 EF hand domains affect Ca^{2+} entry into the mitochondria, which subsequently alter mitochondrial movement. Therefore, it is also plausible that blockage of mitochondrial Ca^{2+} influx by the miro1 EF mutants also contributes to failure in mitochondrial movement arrest in neurons, as reported previously (9–11). Importantly, our findings confirm that intramitochondrial Ca^{2+} is an important determinant of mitochondrial movement, and that there is a critical Ca^{2+} threshold required for pausing mitochondrial movement. Our results differ from a report that examined mitochondrial Ca^{2+} content in cortical neurons using mitochondrial-targeted aequorin protein, in which they found greater mitochondrial Ca^{2+} content in miro1 wild-type and EF hand mutants (9). To ensure this difference is not the result of a difference in population of mitochondria examined (mitochondria in axons versus in soma), we directly examined the fold-change in Ca^{2+} signal in

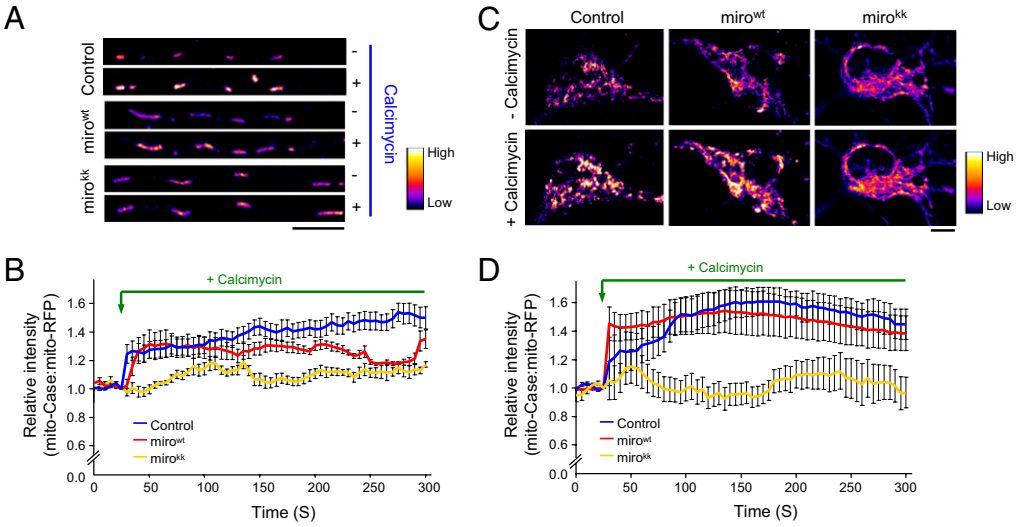

Fig. 4. Mutations in miro1 EF hand domains reduce mitochondrial Ca^{2+} elevation following calcimycin treatment. (*A* and *C*) Representative images of mito-Case12 level (pseudocolored) before and after calcimycin treatment in axon and soma, respectively. (Scale bars, 10 μm.) (*B* and *D*) Mito-Case12:mito-RFP ratio before and after calcimycin treatment in axon and soma, respectively. $Miro^{kk}$ mutant decreased the level of Ca^{2+} entering mitochondria. Values represent mean ± SEM. (*A* and *B*) n = 6 axons each; (*C* and *D*), n = 6 cell bodies each.

the soma following calcimycin treatment. Fig. 4 *C* and *D* shows that $miro^{wt}$ showed similar extent of increase in mitochondrial Ca^{2+} signal compared with the control, but $miro^{kk}$ displayed a diminished level of Ca^{2+} influx compared with control or $miro^{wt}$ constructs, similar to what we observed for mitochondria in axons. Thus, it is possible that differences in the neuronal cell type or detection method gave rise to these different results. However, our results and those by Saotome et al. (9) show that miro1 can alter the level of Ca^{2+} influx into mitochondria.

We further tested whether elevation in mitochondrial Ca^{2+} can override the inhibitory effect of $miro^{kk}$ on mitochondrial movement arrest by treating transfected neurons with SB202190. The levels of mitochondrial Ca^{2+} following SB202190 treatment were similar between $miro^{wt}$- and $miro^{kk}$-transfected neurons, and did not differ significantly from that of the control following SB202190 treatment (i.e., at 1 min after SB202190 treatment, the levels of mitochondrial Ca^{2+} are: control, 1.33 ± 0.10; $miro^{wt}$, 1.24 ± 0.08; $miro^{kk}$, 1.22 ± 0.05) (Fig S11*A*). We found that this increase in mitochondrial Ca^{2+} content significantly decreased mitochondrial movement in both $miro^{wt}$ and $miro^{kk}$, albeit the percentage of moving mitochondria in $miro^{wt}$ and $miro^{kk}$ after SB202190 treatment was still slightly higher than that of the control neurons (Fig. S11*B*). This result is likely caused by a greater percentage of moving mitochondria in $miro^{wt}$- and $miro^{kk}$-transfected neurons before SB202190 treatment. We also found that SB202190 treatment did not change the directionality of moving mitochondria (Fig. S12), consistent with our findings that mitochondrial Ca^{2+} content does not correlate with the direction of mitochondrial movement. Taken together, our results strongly support the hypothesis that intramitochondrial Ca^{2+} content is a crucial determinant of mitochondrial movement and further imply that miro1 may not directly influence mitochondrial Ca^{2+} uniporter opening.

Our findings reveal that mitochondrial matrix Ca^{2+} is an intrinsic signal that actively controls mitochondrial transportation in axons. Although previous reports suggest that cytoplasmic Ca^{2+} modulates mitochondrial movement through miro1 protein, our data argue that mitochondrial matrix Ca^{2+} acts as a gatekeeper of mitochondrial mobility. Blocking mitochondrial Ca^{2+} influx through the mitochondrial uniporter delayed stop in movement, despite intracellular Ca^{2+} elevation, whereas increasing mitochondrial Ca^{2+} alone was sufficient to halt mitochondrial transport. Our live imaging studies show that cytoplasmic Ca^{2+} influx rapidly and invariably leads to mitochondrial Ca^{2+} elevation (as shown by our mito-Case12 imaging studies in Fig. S1), and interestingly, the average speed of mitochondrial movement correlated inversely with mitochondrial Ca^{2+} content. Together with our observation that miro1 EF hand mutant blocked Ca^{2+} entry into the mitochondrial matrix, these results strongly support our conclusion that matrix Ca^{2+} plays an active role in regulating mitochondrial movement, and further suggests that miro1 may have dual roles both in acting as a cytoplasmic Ca^{2+} sensor and in affecting the amount of Ca^{2+} influx into the mitochondria. The molecular components of the mitochondrial Ca^{2+} uniporter are not well understood; but recent studies show that a newly identified 40-kD inner mitochondrial membrane protein is an essential component of the Ca^{2+} uniporter, which also interacts with the MICU1 protein, another inner mitochondrial membrane protein that serves as putative regulator of mitochondrial Ca^{2+} uniporter (27–29). Interestingly, similar to miro1, MICU1 also contains two EF hand domains and a transmembrane domain (29, 30). It is plausible that miro1 may associate with a Ca^{2+}-permeable channel on the outer mitochondrial membrane, such as the mitochondrial voltage-dependent anion channel or other unidentified Ca^{2+} permeable channel, thus influencing Ca^{2+} influx into the mitochondria. It will be interesting in the future to examine the mechanism by which intramitochondrial Ca^{2+} influx through the uniporter in turn affects miro1 interaction with the kinesin motor. As each mitochondrion likely contain multiple miro1 proteins, we speculate that the speed of mitochondrial movement may be regulated by the number of miro1 protein bound to the kinesin motor at a given time, and this miro1-kinesin binding is inversely proportional to the influx of Ca^{2+} into mitochondria. Once intramitochondrial concentration reaches a critical level, all miro1–kinesin interactions are disrupted, and mitochondria therefore stop moving. Studies have shown that mitochondrial Ca^{2+} influx into the mitochondria can stimulate the mitochondrial electron transport chain enzymes and TCA cycle to increase ATP production (14–16); it is thus likely that the high Ca^{2+} concentration inside the stationary mitochondria signals the mitochondria to remain stationary and stimulates the TCA cycle to enhance ATP production, thereby providing energy to the site of high demand. On the other hand, lower Ca^{2+} content in mitochondria may serve as a signal for mitochondria to remain mobile, thus ensuring redistribution to a different location. Taken together, our data are unique in demonstrating that mitochondrial matrix Ca^{2+} content can in-

fluence mitochondrial movement, and further suggest that mitochondria Ca^{2+} can be an intrinsic signal that integrates cellular energy demand and ATP production to actively influence subcellular mitochondrial distribution within neurons.

Materials and Methods

Constructs and Reagents. Mito-RFP used for imaging of mitochondrial movement (pTurboRFP-mito vector) and Case12 protein used for detection of cytoplasmic Ca^{2+} level (pCase12-Cyto vector) were obtained from Evrogen. To detect mitochondrial Ca^{2+} level, a mitochondrial targeting sequence derived from subunit VIII precursor of human cytochrome C oxidase was inserted in the N terminus of the Case12 protein. Localization of mito-Case12 in the mitochondria was confirmed by colocalization with Mito-tracker Red and Mito-RFP. Human wild-type miro1 construct pRK5Myc-Miro1 ($miro^{wt}$) and miro1 EF hand mutations pRK5Myc-Miro1E208K,E328K ($Miro^{kk}$) were obtained from P. Aspenström (Stockholm, Sweden) (9, 11, 31, 32). The following reagents were used: 2 μg/mL calcimycin (3.8 μM; Sigma Aldrich), 10 μM SB202190, and 10 μM RU360 (Calbiochem).

Cell Culture. Mouse hippocampal neurons were obtained from embryonic day 17 to 18 embryos. Dissociated neurons were plated at 40,000 to 55,000 cells on poly-D-lysine–coated glass bottom plates and maintained in neurobasal medium supplemented with B27 and Glutamax (Invitrogen). Neurons were transfected at days in vitro 4 to 5 using Lipofectamine 2000 (Invitrogen) and imaged at days in vitro 7 to 10.

Live Imaging. Hippocampal neurons were imaged in CO_2-independent Tyrode's buffer (referred to as normal extracellular solution) composed of 135 mM NaCl, 5 mM KCl, 1.8 mM $CaCl_2$, 1 mM $MgCl_2$, 10 mM Hepes, 5.6 mM Glucose, pH 7.3 at 37 °C. For experiments done in Ca^{2+}-free solution, Tyrode's buffer was used except 1.8 mM $CaCl_2$ was removed and NaCl changed to 136.8 mM to maintain osmolarity. For experiments done in extracellular solution with low Ca^{2+}, $CaCl_2$ in Tyrode's buffer was changed to 0.18 mM $CaCl_2$, and NaCl changed to 136 mM to maintain osmolarity. Time-lapse images were acquired at 5-s intervals using a Leica SP5 scanning confocal microscope at minimum laser intensity to prevent photobleaching (7–20%) and image-acquisition parameters were set to exclude saturation of signals. Images were acquired for 5 min before and after the addition of 2 μg/mL calcimycin and SB202190 (10 μM). Cells were incubated with RU360 (10 μM) for 15 min before calcimycin treatment.

Imaging Analyses. Fluorescence intensities were measured using ImageJ software and the speed of mitochondrial movement was analyzed using the Manual Tracking Plugin in ImageJ. Dendrites and axons can be distinguished based on morphology, and axons are identified as long, thin processes that extend many times the length of dendrites, which are thicker. To normalize for difference in the size of mitochondria and thus the amount of fluorescent protein inside of mitochondria, as well as photobleaching and shift in focal plane that could occur over time, we normalized mito-Case12 labeling intensity to mito-RFP intensity. To correct for drifts in the *z* axis, cyto-Case12 signals were also normalized to mito-RFP signals. At least three independent transfections per condition were used for imaging analyses. For more details on image analysis, see *SI Materials and Methods*.

Statistics. All values are shown as mean ± SEM, and tested for statistical significance by Student *t* test.

ACKNOWLEDGMENTS. We thank Dr. Aspenström for the generous gift of miro1 constructs used in this work, F. Kennedy for assistance with preparation of hippocampal cell cultures, and the Light Microscopy Imaging Center at Indiana University at Bloomington. This work was supported by Indiana University (K.-T.M.) and Grant NS052524 from the National Institutes of Health (to K.T.C).

1. Hollenbeck PJ, Saxton WM (2005) The axonal transport of mitochondria. *J Cell Sci* 118:5411–5419.
2. Chang DTW, Reynolds IJ (2006) Mitochondrial trafficking and morphology in healthy and injured neurons. *Prog Neurobiol* 80:241–268.
3. Mattson MP, Gleichmann M, Cheng A (2008) Mitochondria in neuroplasticity and neurological disorders. *Neuron* 60:748–766.
4. Hollenbeck PJ (1996) The pattern and mechanism of mitochondrial transport in axons. *Front Biosci* 1:d91–d102.
5. Ligon LA, Steward O (2000) Movement of mitochondria in the axons and dendrites of cultured hippocampal neurons. *J Comp Neurol* 427:340–350.
6. Chada SR, Hollenbeck PJ (2003) Mitochondrial movement and positioning in axons: The role of growth factor signaling. *J Exp Biol* 206:1985–1992.
7. MacAskill AF, Kittler JT (2010) Control of mitochondrial transport and localization in neurons. *Trends Cell Biol* 20:102–112.
8. Cai Q, Sheng Z-H (2009) Mitochondrial transport and docking in axons. *Exp Neurol* 218:257–267.
9. Saotome M, et al. (2008) Bidirectional Ca2+-dependent control of mitochondrial dynamics by the Miro GTPase. *Proc Natl Acad Sci USA* 105:20728–20733.
10. Wang X, Schwarz TL (2009) The mechanism of Ca2+ -dependent regulation of kinesin-mediated mitochondrial motility. *Cell* 136:163–174.
11. Macaskill AF, et al. (2009) Miro1 is a calcium sensor for glutamate receptor-dependent localization of mitochondria at synapses. *Neuron* 61:541–555.
12. Szabadkai G, Duchen MR (2008) Mitochondria: The hub of cellular Ca2+ signaling. *Physiology (Bethesda)* 23:84–94.
13. Kirichok Y, Krapivinsky G, Clapham DE (2004) The mitochondrial calcium uniporter is a highly selective ion channel. *Nature* 427:360–364.
14. McCormack JG, Halestrap AP, Denton RM (1990) Role of calcium ions in regulation of mammalian intramitochondrial metabolism. *Physiol Rev* 70:391–425.
15. Jouaville LS, Pinton P, Bastianutto C, Rutter GA, Rizzuto R (1999) Regulation of mitochondrial ATP synthesis by calcium: Evidence for a long-term metabolic priming. *Proc Natl Acad Sci USA* 96:13807–13812.
16. Chan CS, Gertler TS, Surmeier DJ (2009) Calcium homeostasis, selective vulnerability and Parkinson's disease. *Trends Neurosci* 32:249–256.
17. Vandecasteele G, Szabadkai G, Rizzuto R (2001) Mitochondrial calcium homeostasis: Mechanisms and molecules. *IUBMB Life* 52:213–219.
18. Miller KE, Sheetz MP (2004) Axonal mitochondrial transport and potential are correlated. *J Cell Sci* 117:2791–2804.
19. Verburg J, Hollenbeck PJ (2008) Mitochondrial membrane potential in axons increases with local nerve growth factor or semaphorin signaling. *J Neurosci* 28:8306–8315.
20. Nakai J, Ohkura M, Imoto K (2001) A high signal-to-noise Ca(2+) probe composed of a single green fluorescent protein. *Nat Biotechnol* 19:137–141.
21. Souslova EA, et al. (2007) Single fluorescent protein-based Ca2+ sensors with increased dynamic range. *BMC Biotechnol* 7:37.
22. Csordás G, Hajnóczky G (2003) Plasticity of mitochondrial calcium signaling. *J Biol Chem* 278:42273–42282.
23. Vay L, et al. (2007) Modulation of Ca(2+) release and Ca(2+) oscillations in HeLa cells and fibroblasts by mitochondrial Ca(2+) uniporter stimulation. *J Physiol* 580:39–49.
24. de Jesús García-Rivas G, Guerrero-Hernández A, Guerrero-Serna G, Rodríguez-Zavala JS, Zazueta C (2005) Inhibition of the mitochondrial calcium uniporter by the oxo-bridged dinuclear ruthenium amine complex (Ru360) prevents from irreversible injury in postischemic rat heart. *FEBS J* 272:3477–3488.
25. Montero M, Lobaton CD, Moreno A, Alvarez J (2002) A novel regulatory mechanism of the mitochondrial Ca2+ uniporter revealed by the p38 mitogen-activated protein kinase inhibitor SB202190. *FASEB J* 16:1955–1957.
26. Karahashi H, Nagata K, Ishii K, Amano F (2000) A selective inhibitor of p38 MAP kinase, SB202190, induced apoptotic cell death of a lipopolysaccharide-treated macrophage-like cell line, J774.1. *Biochim Biophys Acta* 1502:207–223.
27. De Stefani D, Raffaello A, Teardo E, Szabò I, Rizzuto R (2011) A forty-kilodalton protein of the inner membrane is the mitochondrial calcium uniporter. *Nature*, 10.1038/nature 10230.
28. Baughman JM, et al. (2011) Integrative genomics identifies MCU as an essential component of the mitochondrial calcium uniporter. *Nature*, 10.1038/nature 10234.
29. Perocchi F, et al. (2010) MICU1 encodes a mitochondrial EF hand protein required for Ca(2+) uptake. *Nature* 467:291–296.
30. Fransson A, Ruusala A, Aspenström P (2003) Atypical Rho GTPases have roles in mitochondrial homeostasis and apoptosis. *J Biol Chem* 278:6495–6502.
31. Reis K, Fransson A, Aspenström P (2009) The Miro GTPases: At the heart of the mitochondrial transport machinery. *FEBS Lett* 583:1391–1398.
32. Fransson S, Ruusala A, Aspenström P (2006) The atypical Rho GTPases Miro-1 and Miro-2 have essential roles in mitochondrial trafficking. *Biochem Biophys Res Commun* 344:500–510.